

Combinatorial explosion in model gene networks

R. Edwards^{a)}

Department of Mathematics and Statistics, University of Victoria, P.O. Box 3045, STN CSC, Victoria, British Columbia V8W 3P4, Canada

L. Glass^{b)}

Centre for Nonlinear Dynamics in Physiology and Medicine, Department of Physiology, McIntyre Medical Sciences Building, McGill University, 3655 Drummond St., Montréal, Québec H3G 1Y6, Canada

(Received 31 January 2000; accepted for publication 16 May 2000)

The explosive growth in knowledge of the genome of humans and other organisms leaves open the question of how the functioning of genes in interacting networks is coordinated for orderly activity. One approach to this problem is to study mathematical properties of abstract network models that capture the logical structures of gene networks. The principal issue is to understand how particular patterns of activity can result from particular network structures, and what types of behavior are possible. We study idealized models in which the logical structure of the network is explicitly represented by Boolean functions that can be represented by directed graphs on n -cubes, but which are continuous in time and described by differential equations, rather than being updated synchronously via a discrete clock. The equations are piecewise linear, which allows significant analysis and facilitates rapid integration along trajectories. We first give a combinatorial solution to the question of how many distinct logical structures exist for n -dimensional networks, showing that the number increases very rapidly with n . We then outline analytic methods that can be used to establish the existence, stability and periods of periodic orbits corresponding to particular cycles on the n -cube. We use these methods to confirm the existence of limit cycles discovered in a sample of a million randomly generated structures of networks of 4 genes. Even with only 4 genes, at least several hundred different patterns of stable periodic behavior are possible, many of them surprisingly complex. We discuss ways of further classifying these periodic behaviors, showing that small mutations (reversal of one or a few edges on the n -cube) need not destroy the stability of a limit cycle. Although these networks are very simple as models of gene networks, their mathematical transparency reveals relationships between structure and behavior, they suggest that the possibilities for orderly dynamics in such networks are extremely rich and they offer novel ways to think about how mutations can alter dynamics. © 2000 American Institute of Physics.

[S1054-1500(00)01103-4]

Tremendous progress has been made in mapping genetic structures in humans and other organisms. This wealth of information will necessitate new analytic tools to deduce function from structure in gene regulatory networks. One way to begin tackling this problem is to investigate simple idealized switching networks that capture the various possible logical structures of real gene networks (or other networks characterized by strong switching). Discrete-time Boolean switching networks have been used for this purpose, but we study model networks that are continuous in time, represented by differential equations, though interactions between genes are still modeled by Boolean functions. Steady states and simple stable oscillations have been shown to

exist in networks of this type with 3 genes and it is known that more than one pattern of oscillation is possible with 4 genes, as well as irregular behavior. We show here that there is actually a combinatorial explosion of different logical structures possible as the number of genes increases and a corresponding explosion of dynamical possibilities. Even with only 4 genes, at least hundreds of different stable periodic patterns are possible, some of them surprisingly long and complex. The existence of these stable periodic behaviors is proven analytically, though we searched for these cycles by numerically integrating solution trajectories in a million randomly generated network structures. The results and methods of this study provide a way to organize thinking about the relation between structure and function as well as the effects of mutation in real gene networks whose structures are being revealed by current research. They also suggest that the range of possibilities for orderly dynamics in gene networks is extraordinarily rich.

^{a)}Electronic mail: edwards@math.uvic.ca

^{b)}Electronic mail: glass@cnd.mcgill.ca

I. INTRODUCTION

The explosive growth in knowledge of the sequence of the nucleotides in the genome of humans and other organisms leaves open the question of how the functioning of the genes is coordinated to lead to orderly development and orderly function. New technologies, including gene expression chips that enable one to determine simultaneously the activities of thousands of genes, promise to expand greatly our information concerning the coordinated function and dynamics of networks of genes.^{1,2} It seems likely that mathematical techniques, of comparable power and generality to the new experimental methods, will be essential to interpret and codify the expanding data.

Two complementary mathematical approaches have emerged. In one, detailed mathematical models are developed for comparatively well-defined genetic networks. For example, mathematical models have been proposed for the genetic circuits in lambda bacteriophage,^{3,4} drosophila development,⁵ and *arabidopsis*.⁶ A second approach is to study mathematical properties of abstract models of genetic networks, often with a focus on global properties of the dynamics of a class of models rather than an analysis of how any particular organism works. For example, an early idealization of genetic networks as discrete time Boolean networks,^{7,8} led to the recognition that statistical aspects underlying the structure of a network, such as the number of gene products that affect the expression of any given gene, have important consequences for the dynamics of the entire network. The key issue unifying both approaches is to understand how some particular type of behavior can be generated by a genetic network.

Since real organisms do not have discrete clocking devices such as are hypothesized in switching network models, most attempts at realistic modeling of genetic networks formulate the models as differential equations.^{3-5,9} The variables in the differential equations represent levels of gene activity, for example, as monitored by levels of nucleic acids or proteins coded by specific genes. Gene activities are regulated by a large variety of circulating factors. It is common for biologists to imagine that genes are switched "on" or "off," depending on the levels of factors regulating each particular gene. Consequently, one can imagine that a logical structure underlies a differential equation modeling a gene network.

An idealized class of differential equations makes explicit the logical structure.¹⁰ These equations have certain mathematical properties that make them amenable to mathematical analysis: (i) the equations are piecewise linear, and can be integrated accurately and rapidly;¹⁰ (ii) the piecewise linear flows lead to dynamics described by the composition of fractional linear maps (see definition below) facilitating analysis of periodic^{11,12} and chaotic dynamics;¹³⁻¹⁵ (iii) the underlying logical structure and the resulting dynamics are both related to a directed graph on an n -dimensional hypercube (n -cube), inviting classification of the possible network structures.^{10,16} For example, in Fig. 1 we show the directed hypercube representation for two different networks.^{10,17} Figure 1(a) shows the 2-cube representing a network in which 2

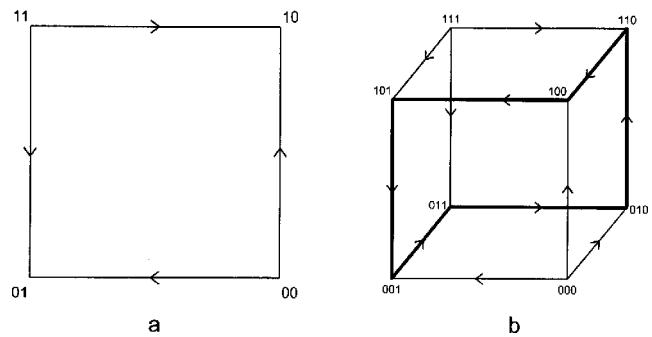


FIG. 1. (a) Hypercube structure of a 2-net with two stable fixed points. Vertices corresponds to states of the system, so, e.g., "10" represents the state in which the first gene's product is above the threshold concentration where its presence is felt by the other gene, while the second is below its threshold. (b) Hypercube structure of a 3-net with a cyclic attractor marked by bold lines. Again, vertices correspond to states (gene product concentrations above or below threshold).

model genes mutually inhibit the production of each other. In this case there are two steady states, represented by the vertices 10 and 01. The vertex labels correspond to states (concentrations) of the gene products, so "10" means that the first gene's product is above the threshold where its presence is felt by the other gene, while the second is below its threshold. Figure 1(b) shows a 3-cube for a network in which there are 3 model genes. The first gene inhibits production of the third, and the second inhibits production of the first. In this network there is a cycle through the six states $100 \rightarrow 101 \rightarrow 001 \rightarrow 011 \rightarrow 010 \rightarrow 110 \rightarrow 100 \dots$. The approach blends concepts from combinatorics and nonlinear dynamics. These dynamics appear both in the digraphs on the n -cubes, as well as in differential equations that model these networks.

The following question underlies much of this work: *Given a network with a certain logical structure (or equivalently, a certain directed graph on an n -cube), what are the possible dynamics that can be found in this network?* For networks with 2 and 3 variables, there can only be steady states and limit cycles and the numbers of different networks is comparatively small (4 in 2 dimensions and 112 in 3 dimensions).¹⁰ For 4 dimensions, in addition to steady states and limit cycles, chaotic dynamics is possible.¹³⁻¹⁵ However, previous work did not address the total number of different networks in 4 or higher dimensions and only identified a restricted class of limit cycles.

The current work investigates dynamics in the highly simplified model gene networks proposed by Glass.¹⁰ We show that even in networks with 4 interacting genes, large numbers of distinct logical structures are possible leading to a correspondingly rich dynamics. In Sec. II, we present the equations and give their main properties. In Sec. III, we develop the combinatorial methods to count the number of different networks in a given dimension. Section IV summarizes methods that have been developed to analyze the flows in any given network using fractional linear maps. Section V presents a numerical study of random networks in 4 dimensions and shows that there are a large number of different cycles present in these networks. Section VI describes ways in which different cycles may be related to each other. Fi-

nally, in Sec. VII we discuss the relevance of this work to biology and mention several questions that are left open by the analysis.

II. PIECEWISE LINEAR EQUATIONS FOR MODEL GENE NETWORKS

Glass proposed¹⁰ that complex biological networks, such as gene networks, can be classified in terms of an underlying “deep structure” of the dynamics represented by a state transition diagram. The state transition diagram for a system of n interacting quantities (which we will call an n -net) is a directed graph (digraph) on an n -cube, in which vertices correspond to orthants (the n -dimensional generalization of quadrants or octants) of state space and transitions along edges between vertices correspond to flow across boundaries between adjacent orthants. In general, this structure applies to any system of n ODEs whose state space can be decomposed into 2^n regions homeomorphic to the 2^n orthants of \mathbf{R}^n , and for which flows from one region to another are in one and only one direction.¹⁶ This structure emerges naturally from model systems representing switching networks in continuous time,

$$\dot{y}_i = -y_i + F_i(\tilde{y}_1, \tilde{y}_2, \dots, \tilde{y}_n), \quad i = 1, \dots, n, \quad (1)$$

where

$$\tilde{y}_i = \begin{cases} 0 & \text{if } y_i < 0 \\ 1 & \text{if } y_i > 0 \end{cases} \quad (2)$$

We think of y_i as a protein product (transcription factor) produced by gene i , that may act to regulate the rates of production of other gene products through the piecewise constant functions F_i . Systems with a step function at threshold values other than 0 reduce to the above equations without loss of generality. From the point of view of our later analysis, decay rates that depend on $\tilde{\mathbf{y}} = (\tilde{y}_1, \tilde{y}_2, \dots, \tilde{y}_n)'$ (the ' denotes the matrix transposition) are manageable by the same techniques as long as the decay rates are uniform across variables at any given time. The piecewise linear functions facilitate analysis, but substitution of sigmoidal control for step function control in simple networks leads to equivalent dynamics.^{10,17,18} Furthermore, there is a more general result that, at least under some conditions, if a limit cycle exists in a network with steep sigmoids as the “gain” (slope) of the sigmoids increases, then it persists all the way to the step function limit.¹⁹

Since for the system specified by Eqs. (1) and (2) there are a finite number of values F_i (in fact, $n2^n$ of them), it is clear that solutions are globally bounded. In order to guarantee that the flow across boundaries of orthants in phase space is unambiguously directed, we will impose two additional conditions:

Condition 1: $F_i(\tilde{\mathbf{y}}) \neq 0, \forall i, \forall \tilde{\mathbf{y}}$, and

Condition 2: $F_i(\tilde{y}_1, \dots, \tilde{y}_i = 0, \dots, \tilde{y}_n) = F_i(\tilde{y}_1, \dots, \tilde{y}_i = 1, \dots, \tilde{y}_n), \forall i, \forall \tilde{\mathbf{y}}$.

Condition 2 states that F_i does not depend on y_i , i.e., that there is no self-input in the network. In fact a weaker condition suffices to ensure unambiguous flow across boundaries,

namely that $\text{sign}(F_i)$ does not depend on y_i . Since the directions of flows across orthant boundaries (equivalently across edges in the state transition diagram) depend on the signs of the F_i 's, there is a particularly simple network corresponding to each state transition diagram; the one for which $F_i(\tilde{\mathbf{y}}) = \pm 1$ for every i and $\tilde{\mathbf{y}}$. For these networks, each F_i is a Boolean function [we could equivalently have taken $F_i = 0$ or 1 if we had used a threshold of $\frac{1}{2}$ in Eq. (2)]. As we show below, the values of F_i define focal points in state space, where the flows at any time are directed towards a focal point determined by the current orthant of state space. Although it is a major question to determine the different possible dynamics as a function of the position of the focal points for a given state transition diagram, in the current paper unless otherwise stated we assume that all focal points lie at vertices of the unit hypercube, i.e., $F_i = \pm 1$.

Another important subclass of Eq. (1) arises when $F_i = \sum_{j=1}^n w_{ij} \tilde{y}_j - \tau_i$. These have the form of additive neural networks, where w_{ij} is the connection weight between neurons j and i and τ_i is the threshold of neuron i . Such equations occur, for example, in Hopfield networks.²⁰

The state transition diagrams can be used to define “structural equivalence classes” for switching networks; two networks are in the same class if their state transition diagrams are the same, up to symmetry transformations on the n -cube. Note that while each state transition diagram corresponds to exactly one Boolean switching network, several of these may still be in the same equivalence class due to the symmetries of the n -cube. If we allow the focal point coordinates to deviate from ± 1 , then the qualitative dynamical behavior of networks in the same structural equivalence class is not necessarily the same, but the structure does impose constraints on the possible dynamics and some results relating structure to dynamics have been obtained. If a vertex has all adjacent edges pointing inward then there is a fixed point of the network dynamics in the corresponding orthant (once a trajectory enters this orthant, it cannot leave and must converge to $\mathbf{F}(\tilde{\mathbf{y}})$, where $\mathbf{F} = (F_1, F_2, \dots, F_n)'$). Furthermore, Glass and Pasternack¹¹ proved that if the state transition diagram has a “cyclic attractor” (a cycle for which all adjacent edges point towards the cycle) then the network either has a stable periodic orbit corresponding to this sequence of transitions, or its orbits spiral in to the origin. For example, there are two stable steady states for the network represented in Fig. 1(a). In this and subsequent n -cube diagrams, vertices correspond to quadrants (orthants) of phase space, and are labeled according to $\tilde{\mathbf{y}}$, the sign structure of the quadrant (orthant), and directed edges show the direction of flow across boundaries between orthants. One network with the structure of Fig. 1(a) (the Boolean one) is defined by the focal points listed in Table I(a). To see how the digraph is obtained from the focal points, consider the first line of the table, for example, $F(0,0) = (1,1)$. When $y_1 < 0$ and $y_2 < 0$ the focal point has both coordinates positive and the possible transitions are to $\tilde{\mathbf{y}} = (1,0)'$ or $(0,1)'$, depending on which variable becomes positive first. Thus, on the digraph, we direct the edges $00 \rightarrow 01$ and $00 \rightarrow 10$. Table Ib defines a network with the structure of Fig. 1(b) and this has a cyclic

TABLE I. Focal points, $F(\tilde{y})$, for networks that correspond to the structure of (a) Fig. 1(a), and (b) Fig. 1(b). The networks are defined by Eqs. (1) and (2).

		(a)		
\tilde{y}		$F(\tilde{y})$		
0 0		1	1	
0 1		-1	1	
1 0		1	-1	
1 1		-1	-1	
		(b)		
\tilde{y}		$F(\tilde{y})$		
0 0 0		1	1	1
0 0 1		-1	1	1
0 1 0		1	1	-1
0 1 1		-1	1	-1
1 0 0		1	-1	1
1 0 1		-1	-1	1
1 1 0		1	-1	-1
1 1 1		-1	-1	-1

attractor that leads to a stable limit cycle, shown in Fig. 2.

The number of possible cyclic attractors (up to symmetries) in directed graphs on the 3-cube, 4-cube, and 5-cube have been counted.¹⁶ There is only one for the 3-cube, there are 3 for the 4-cube, and 18 for the 5-cube. For the situation in which $F_i = \pm 1$ the cyclic attractors in dimension 3 and higher imply limit cycles in Eq. (1). Moreover, in dimension 3, 4, and 5, each different cyclic attractor corresponds to a limit cycle with a distinct period. From the early work on these networks, three different types of stable behavior (attractors) were known for $n=3$; a limit cycle corresponding to the cyclic attractor, a fixed point (stable node) in the interior of an orthant and a fixed point on a coordinate axis or at the origin (focus). For $n=4$, a similar set of behaviors was known, except that three structurally different cyclic attractors and therefore geometrically different stable periodic orbits are possible. Since then, numerical experiments with randomly generated networks have shown that the range of possible behaviors for $n \geq 4$ is much richer than was realized in the early work.^{13,14,20,21}

In order to explore the range of possible behaviors in 4-nets, we ask the following questions. First, how many structural equivalence classes are there for an n -net? This gives an idea of the size of the space we are investigating. Then, what types of behavior are possible for 4-nets, particu-

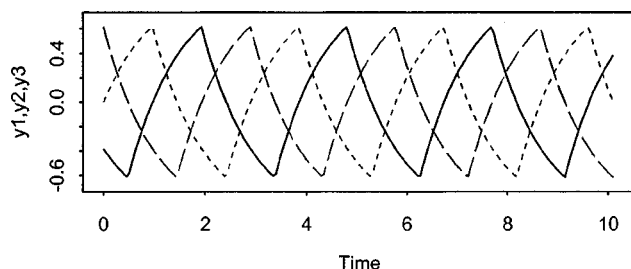


FIG. 2. Limit cycle for the network in Table I(b) and Fig. 1(b). The period is 2.8872710. The activity of all three units is shown; the units of time and activity are arbitrary.

larly patterns of oscillation, or periodic orbits? To answer this question partially, we summarize techniques of analysis^{12,13,15} and report on our numerical investigations which include analytic confirmation of the existence of every periodic orbit discovered.

III. COMBINATORIAL BOUNDS

In this section we compute the number of structural equivalence classes for n -nets. An n -cube has $E(n) = n2^{n-1}$ edges and there are 2 choices of direction on each edge, so without considering symmetries there are $2^{E(n)}$ different directed graphs. However, many of these correspond to each other via symmetry transformations, such as rotations, reflections and relabelings. Glass¹⁶ used Burnside's lemma^{22,23} to show that of the $2^{12} = 4096$ possible directed graphs on the 3-cube, there are only 112 structural equivalence classes.

Let U be the set of directed graphs on the n -cube. Let $c(n)$ be the number of equivalence classes of such graphs where the equivalence relation is defined by the group of symmetry transformations, $T_i, i = 1, \dots, m$, which do not alter the essential network structure. Let $I(T_i)$ be the number of elements of U left invariant by symmetry transformation T_i . Then Burnside's lemma states that

$$c(n) = \frac{1}{m} \sum_{i=1}^m I(T_i). \tag{3}$$

For the 2-cube, for example, there are $2^4 = 16$ elements in U . The 4 rotations and their reflections give $m = 8$ symmetry transformations. The identity transformation, T_1 , always leaves every element of U invariant, so $I(T_1) = 16$. The others leave 0, 2, or 4 directed graphs invariant and the sum in Eq. (3) is $(1 \cdot 16) + (3 \cdot 4) + (2 \cdot 2) + (2 \cdot 0) = 32$. Thus, $c(2) = 32/8 = 4$. Similar arguments allow one to count the equivalence classes for the 3-cube. It becomes difficult to visualize the symmetry transformations, however, for $n \geq 4$.

Systematic combinatorial approaches have been developed for problems of this nature. The symmetry group for the n -cube is isomorphic to the hyperoctohedral group O_n .²² The number of symmetry transformations for this group is $m(n) = n!2^n$. One way to count these symmetries is to see that there are 2^n choices for where a given vertex will be taken under a transformation and then $n!$ ways of permuting the adjacent edges.

The problem of counting the number of distinct digraphs on the n -cube is related (through the symmetry group) to that of counting the number of 2-colorings on the vertices of the n -cube, or equivalently, the number of Boolean functions of n variables.^{22,24} This problem was solved²² by building on methods due to Pólya in which the cycle polynomial and cycle index polynomial code information about the cycle structures of the group of transformations. Chen²⁵ has extended this result to that of edge-colorings of the n -cube. However, the equivalence relation implied by 2-colorings of the edges is not the same as that implied by digraphs. Consider, for example, reflection of the 2-cube (square) in a vertical line. There are eight 2-colorings of the edges that are left invariant under this transformation (the left and right

edges need only be the same color) but no digraph can be invariant since the top and bottom edges will have their directions reversed.

A good intuition about the problem of counting the number of distinct configurations under the symmetries of the directed n -cube can be obtained by computing a lower bound on the number of different configurations. Suppose each symmetry operation of the n -cube generated a distinct configuration of directed edges on the n -cube. Then the total number of distinct structural equivalence classes, $c(n)$, would be the total number of configurations of the directed n -cube divided by the number of symmetry operations in O_n . In other words, if none of the configurations are identical under a symmetry of the cube, then the number of symmetry operations times the number of different classes equals the total number of digraphs. However, since some symmetry operations leave the graph unchanged, we obtain

$$c(n) > \frac{2^{n2^{n-1}}}{n!2^n}. \tag{4}$$

The inequality arises because not all symmetry operations of the n -cube necessarily generate a distinct configuration for any particular directed graph. However, as we will see, this lower estimate is amazingly accurate as the number of dimensions increases.

We now consider the exact computation of $c(n)$. Since a closed-form solution has apparently not yet been obtained, we take a more direct, computational approach. Essentially, the problem boils down to counting the cycles induced by each symmetry transformation in O_n . The number of invariant digraphs under a transformation will be 2^d , where d is the number of cycles, because there is only one choice of orientation for each cycle (after the orientation of the first edge is decided, the other edges of the cycle are fixed). In the Appendix, we outline our method of counting these cycles via an algorithm that traverses them, and then apply Burnside's lemma to obtain the result, which can be written

$$c(n) = \frac{1}{m(n)} \sum_d \nu(d)2^d = \frac{\sum_d \nu(d)2^d}{n!2^n}, \tag{5}$$

where $\nu(d)$ indicates the number of transformations generating exactly d cycles.

For $n=3,4,5$ the counts $\nu(d)$ are shown in Table II. The lower bound computed in Eq. (4) is the largest term in Eq. (5), i.e., the one with the largest value of d , corresponding to the identity transformation.

For larger n these tables are easy to compute, but the numbers quickly become very large. The number of distinct digraphs (equivalence classes) on the n -cube [from Eq. (5)] for $n=1$ to 5 is given in Table III.

As a consequence of these calculations, we can say that the random sample (with replacement) of a million 4-cube structures reported below does not come close to exhausting the full set of 11 223 994 equivalence classes. The combinatorial explosion of structural equivalence classes leaves plenty of room for many different limit cycles, though it does not give a clear indication of how many there are. Not all structures will have stable limit cycles.

TABLE II. Numbers of transformations of digraphs on the n -cube ($n=3,4,5$) leaving d choices of edge orientation to ensure invariance under the transformation. Totals include transformations that leave no digraph invariant.

$n=3$		$n=4$		$n=5$	
d	$\nu(d)$	d	$\nu(d)$	d	$\nu(d)$
2	8	4	48	8	704
3	12	6	64	10	480
4	8	8	132	16	944
6	4	12	32	20	680
7	6	16	35	22	240
12	1	20	12	32	80
		32	1	40	106
				42	60
				52	20
				80	1
total	48	total	384	total	3840

There are other factors influencing the variety of limit cycles. If a periodic orbit exists for the network, then it must follow a cycle of edges on the n -cube. The converse is not necessarily true, however (see Sec. IV). Bistability or multistability also occurs in some networks (Sec. V).

Furthermore, a given cycle structure, taking into account the pattern of adjacent edges pointing toward or away from the cycle, can occur on different hypercubes, since edges other than those adjacent to the cycle can vary without affecting the cycle.

IV. ANALYSIS

The analysis of continuous-time switching networks was begun by Glass and Pasternack¹¹ and was further developed mainly by Mestl, Plahte, and Omholt,¹² Mestl, Lemay, and Glass,¹³ and Edwards.¹⁵ What follows is a brief summary of this work.

The main property of continuous-time switching networks that makes them tractable is that trajectories are piecewise linear. For $\mathbf{y}=(y_1, y_2, \dots, y_n)$ in one orthant of phase space (and therefore with one fixed sign structure) the solution to Eq. (1) in vector form is

$$\mathbf{y}(t) = \mathbf{f} + (\mathbf{y}(0) - \mathbf{f})e^{-t}, \tag{6}$$

which describes exponential approach to $\mathbf{f}=(f_1, f_2, \dots, f_n)=\mathbf{F}(\tilde{\mathbf{y}})$. The trajectory in n -dimensional state space is a straight line between $\mathbf{y}(0)$ and $\mathbf{F}(\tilde{\mathbf{y}})$. Thus, each orthant of phase space (with sign structure $\tilde{\mathbf{y}}$) has an associated focal point, \mathbf{f} , somewhere in \mathbf{R}^n . If trajectories in

TABLE III. Numbers of distinct digraphs on the n -cube, considering symmetries.

n	$c(n)$	Lower bound
1	1	1.000
2	4	2.000
3	112	85.333
4	11 223 994	11 184 810.666
5	314 824 455 746 718 261 696	314 824 432 191 309 680 913.066

an orthant are directed to a focal point \mathbf{f} within that orthant then once the orthant is entered no further switchings take place and \mathbf{f} is a stable fixed point of the network dynamics. Otherwise, trajectories are formed of piecewise linear segments between orthant boundaries, with corners at the boundaries. Under Condition 2, there is no ambiguity in the direction of flow across an orthant boundary so trajectories are well defined there. Thus, given a point on an orthant boundary, it is possible simply to calculate the next orthant boundary crossing point directly, and to integrate along trajectories it is only necessary to repeat this process at each step.

We now denote by $\mathbf{y}^{(k)}$ the k th orthant boundary crossing on a trajectory and assume that $\mathbf{f}^{(k)}$, the focal point associated with the orthant being entered, does not lie in that orthant. The map from one boundary to the next can be represented as an operator ($M^{(k)}: \mathbf{R}^n \rightarrow \mathbf{R}^n$),

$$\mathbf{y}^{(k+1)} = M^{(k)} \mathbf{y}^{(k)} = \frac{B^{(k)} \mathbf{y}^{(k)}}{1 + \langle \psi^{(k)}, \mathbf{y}^{(k)} \rangle}, \tag{7}$$

$$B^{(k)} = I - \frac{\mathbf{f}^{(k)} \mathbf{e}_j'}{f_j^{(k)}}, \quad \psi^{(k)} = \frac{-\mathbf{e}_j}{f_j^{(k)}},$$

where j is the variable that switches at the k th step, \mathbf{e}_j denotes the standard basis vector in \mathbf{R}^n , and the angle brackets denote the Euclidean inner product ($\langle \psi, \mathbf{y} \rangle = \psi^T \mathbf{y}$). Thus, $M^{(k)}$ is a fractional linear map with a vector numerator and scalar denominator. The composition of such maps is again a fractional linear map of the same form. Also, since these maps are between orthant boundaries where one of the y_i 's is always 0, they can be reduced by one dimension, by removing the appropriate row and column in each $B^{(k)}$, $\mathbf{y}^{(k)}$, and $\psi^{(k)}$. For a cycle (a trajectory that returns to its initial orthant boundary), we arrive at (dropping the superscripts)

$$M \mathbf{y} = \frac{A \mathbf{y}}{1 + \langle \phi, \mathbf{y} \rangle}, \tag{8}$$

where A is $(n-1) \times (n-1)$, $\phi \in \mathbf{R}^{n-1}$ and $\mathbf{y} \in \mathbf{R}^{n-1}$. We call M the return map. This discrete map, along with the crossing times, contains all information in the full continuous-time dynamics.

We now list without proof key properties of the cycle map M [Eq. (8)] and corresponding periodic orbits.

Along a cycle on the n -cube, there may be branching vertices, i.e., vertices with more than one outgoing edge. These correspond to orthants from which trajectories can exit by more than one boundary hyperplane, depending on which variable reaches zero first. Alternative exit variables impose constraints on the region of an orthant boundary that maps forwards through a specified sequence of boundaries. These constraints take the form of linear inequalities, and the restricted regions are the interiors of ‘‘proper cones’’ (Ref. 26 p. 6).

Proposition 1: Given an n -cube cycle and initial orthant boundary, \mathcal{O} , the cone from which trajectories follow the cycle and return to \mathcal{O} is given by

$$C = \{ \mathbf{y} \in \mathcal{O} | R \mathbf{y} \geq 0 \}, \tag{9}$$

where R is a matrix with one row for each alternative exit variable, $y_i^{(k)}$, around the cycle, each row being

$$R_{i,\cdot} = - \frac{\mathbf{e}_i'}{f_i^{(k)}} B^{(k)} B^{(k-1)} \dots B^{(0)}. \tag{10}$$

We allow equality, $R \mathbf{y} = 0$, as a limiting case. These are trajectories for which two variables cross their thresholds simultaneously. Many of the inequalities generated by Eq. (10) will be redundant and can be weeded out in computation.

The domain of definition of the return map, M is only $C \subset \mathcal{O}$. Trajectories starting outside of C , but in \mathcal{O} , eventually branch away from the given cycle. Note also that M maps C into \mathcal{O} , not necessarily into C . However, a fixed point of the map lying inside C continues to return and corresponds to a periodic orbit for the differential equations. If C is empty, no periodic orbit corresponding to this n -cube cycle exists.

The following result establishes that fixed points of M lie on eigenvectors of A , gives criteria for their existence and allows calculation of their location.

Proposition 2: Any nonzero (real) fixed point of M [Eq. (8)] in C is a (real) eigenvector of A corresponding to an eigenvalue > 1 . Conversely, if \mathbf{v} is a real eigenvector of A with eigenvalue $\lambda > 1$, and $\mathbf{v} \in C$, then

$$\mathbf{y}^* = \frac{(\lambda - 1) \mathbf{v}}{\langle \phi, \mathbf{v} \rangle} \tag{11}$$

is a fixed point of M , unique in the span of \mathbf{v} . If $\lambda = 1$, then the only fixed point in the span of \mathbf{v} is $\mathbf{0}$.

The stability of a fixed point of M depends on the corresponding eigenvalue of A being dominant.

Proposition 3: A fixed point, \mathbf{y}_i^ , of M corresponding to the eigenvalue λ_i of A , is asymptotically stable if $\lambda_i > |\lambda_j|$, $\forall j \neq i$, neutrally stable if $\lambda_i \geq |\lambda_j|$, $\forall j \neq i$, but equality holds for some j , and unstable otherwise.*

This is proved by the standard linearization (Jacobian) at the fixed point. When A has real, distinct eigenvalues at least, lines between fixed points of M are their stable and unstable manifolds, and the eigenvalues of the Jacobian are ratios of eigenvalues of A .

Proposition 4: A periodic orbit with cycle map M has period $P = \log(\lambda)$, where λ is the eigenvalue of the matrix A associated with the fixed point on the orbit.

The proof of this result¹⁵ depends on the demonstration that the denominator in the map [Eq. (7) or (8)] for any sequence of trajectory segments is the exponential of the time taken to traverse them. Since the denominator at a fixed point of the map is also the associated eigenvalue of the matrix A , the log of this eigenvalue is the period of the corresponding periodic orbit.

Thus, given a network and a cycle on its n -cube, it is possible to determine the existence, stability and period of any associated periodic orbit explicitly, and these calculations can be automated, so that many cycles can be checked quickly. The procedure is as follows.

- (1) Select an orthant boundary on the cycle to start from.

- (2) Calculate the return map [Eq. (8)] from the composition of fractional linear mappings corresponding to the sequence of orthants traversed from the starting orthant boundary.
- (3) Find the eigenvalues and associated eigenvectors of the matrix A in the return map.
- (4) For real eigenvalues $\lambda > 1$, calculate the fixed points on the corresponding eigenvectors from Eq. (11).
- (5) Calculate the returning cone, C , for the return map from Eq. (9), if it is nonempty.
- (6) If a fixed point of the map lies in C , then it corresponds to a periodic orbit. In this case if its eigenvalue is the (unique) dominant one then the periodic orbit is asymptotically stable; if the modulus of other eigenvalues as well as this one attain the spectral radius, the orbit is neutrally stable; otherwise it is unstable. If the fixed point lies on the boundary of C then the periodic orbit is “degenerate,” in the sense that two variables switch simultaneously.

V. RANDOM SAMPLE OF A MILLION NETWORKS

To search for behaviors in 4-nets with focal points at ± 1 , a million 4-cube structures were randomly generated (with the no-self-input restriction, Condition 2). Each was numerically integrated from a random initial condition for a maximum of 36300 steps (less if convergence was detected earlier—the results of the integration were checked after several stages of increasing length to catch fast convergence sooner). If a fixed point within an orthant was reached, integration stopped. Otherwise, the switching sequence, defined to be a sequential listing of the index i of the variable \tilde{y}_i that switches, was examined for periodic behavior. Periodic behavior is identified as a cycle of switching variables in which every variable switches an even number of times (so, e.g., the sequence 1-2-1-4 would not be counted as a cycle, but 1-2-1-4-1-2-1-4 would). If the end of the full sequence consisted of at least three repetitions of such a cycle, the cycle was considered a candidate for a periodic orbit. Cycles of as many as 7290 switchings were searched for and would have been found by the program. All such candidate cycles were further checked for convergence of the values of the variables after each circuit. If all variables returned to within 10^{-10} over the last circuit of the cycle, the cycle was retained as a candidate for a periodic orbit, otherwise the integration was continued or if the length of integration had reached its maximum the network was stored for closer inspection manually. Cycles of 2 or more variables switching with cycle times that decreased but did not converge were considered to be trajectories spiraling in to a fixed point and were not pursued further. (It is possible that such a trajectory could be misclassified if it is actually converging very slowly towards a cycle, but slow convergence does not occur in networks in the current situation.) Integration was also stopped when two variables switched at the same time (within 10^{-15} time units). This was taken to be an indication of convergence to a cycle that in fact involved two variables switching together (see below).

Cycles obtained by the numerical integration as candi-

TABLE IV. Numbers of randomly generated 4-nets with the five possible behavior classes.

nodes	555633
foci	435410
periodic orbits (nondegenerate)	5668
periodic orbits (degenerate)	2654
irregular	635
Total	1000000

dates for periodic orbits were then checked according to the procedure outlined in Sec. IV. Given the hypercube structure (i.e., the set of focal points) and the proposed cycle of orthants (determined by the starting boundary and the switching sequence), the return map was calculated and the eigenvectors and eigenvalues of the A matrix, as well as the fixed points of the map. Then the returning cone was calculated, and the fixed point associated with the dominant eigenvalue checked to see whether it was in the returning cone. Thus, we did not rely on the numerical integration as evidence of periodicity, rather we used it to suggest candidate cycles which were then verified analytically by checking that they satisfied the conditions of the result in Sec. IV.

In no cases did we find that a candidate cycle was rejected by this verification process. However, in some cases, the fixed point of the return map fell exactly on the boundary of the returning cone (sometimes on the boundary of the orthant boundary itself, indicating that two variables switch together), within an epsilon to account for roundoff error. Trajectories following these “degenerate” cycles follow an unambiguous sequence of switchings but converge towards an ω -limit set in which two variables switch together. There is in this case a possibility of ambiguity if the trajectory near the double-switching depends sensitively on which of the two switches first. In that case the ω -limit set is not a limit cycle, since a small perturbation on one side leads the trajectory away. These are nevertheless identified by the program as periodic orbits. In some cases of degenerate cycles, the approaching trajectory follows two different subcycles of switchings in alternation, both subcycles approaching the same degenerate limiting cycle. In such cases the limiting cycle is taken as one circuit, not the two (now identical) subcycles, and the period is half what the approaching cycle (consisting of both subcycles) would suggest.

This numerically based but analytically verified search for stable periodic orbits in different 4-net structures produced a huge variety of possibilities. Of course, many networks are identical to others under symmetry transformations (rotations, reflections, relabelings) so apparently different hypercube cycles may not be genuinely different. Cycles identical except for a symmetry transformation, however, must at least have the same period and length of switching sequence. The break-down of behaviors found in the 1000000 simulations are listed in Table IV.

Those for which no convergence was detected were classified as irregular. There is, of course, no proof from the above that these would not eventually converge to a fixed point or a periodic orbit, but investigation of some examples suggests that they are in fact chaotic.^{14,15}

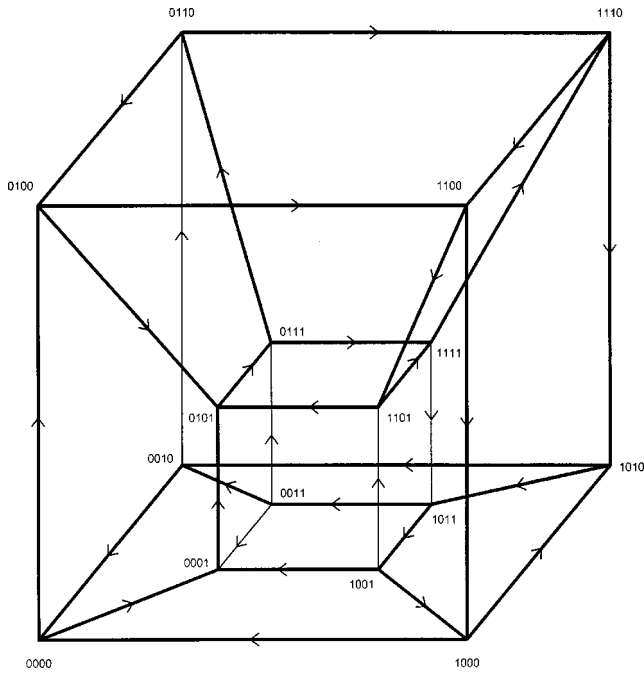


FIG. 3. Hypercube structure of a 4-net with a periodic orbit following a cycle of length 174. The edges traversed by the cycle are marked by bold lines.

Of the 1000000 random networks, 8322 converged to periodic orbits. In order to determine how many truly different cycles there are amongst these, we would need to compare the switching sequences and the patterns of alternate exit variables along the cycles, considering symmetries. We can classify in a courser way, however, using simply the period of the orbit, noting that one period can be associated with many different switching sequences, even sequences of different lengths. Among the 8322 periodic orbits we found 301 different periods. The shortest period was 1.4436355 time units associated with switching sequences of length 8 or more. The shortest switching sequence is the one of length 6 that occurs in the 3-element network represented by the 3-cube in Fig. 1(b), and has period ≈ 2.8872710 (Fig. 2). Earlier analysis shows that this period is exactly $6 \ln((1 + \sqrt{5})/2)$.^{15,16} This was also the most commonly occurring period, accounting for 2464 of the 8322 periodic orbits. The longest period was 62.7563895 for a cycle of length 252, which was also the longest switching sequence.

It is surprising that such simple networks with only 4 elements can produce such a huge variety of different stable periodic orbits, including some with sequences of up to 252 switchings. The trajectories of these long limit cycles are also quite varied in appearance, in amplitude, and period. For

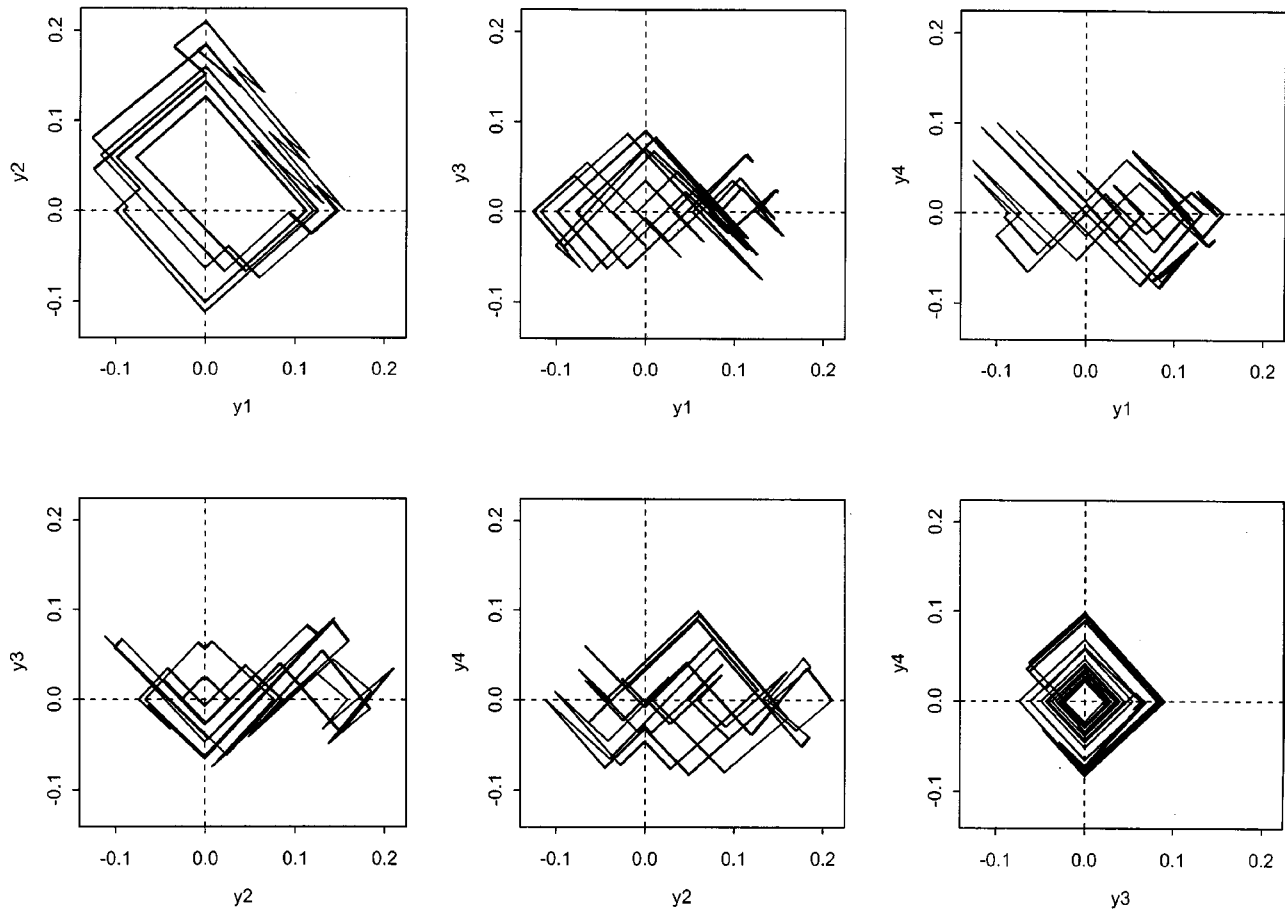


FIG. 4. Phase space projections of a periodic orbit with switching sequence of length 174 on the 4-net of Fig. 3.

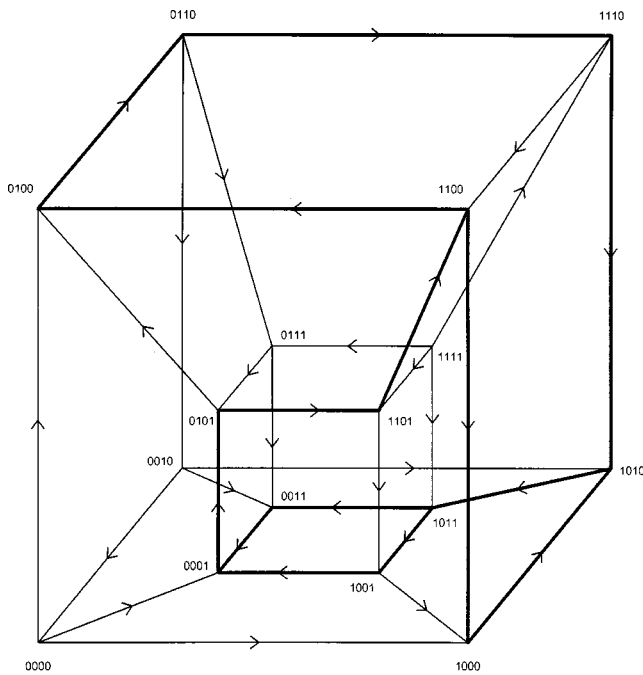


FIG. 5. Hypercube structure of a 4-net with a periodic orbit following a cycle of length 110. The edges traversed by the cycle are marked by bold lines.

example, one limit cycle consisting of 174 switchings (Figs. 3 and 4) has a period of only 6.1517884 and has very small amplitude, whereas another of length 110 (Figs. 5 and 6) has period 22.1535440 and an amplitude comparable to those of most shorter cycles. Furthermore, the basins of attraction of these long-period (and long switching sequence) orbits appear to be large: Many initial conditions lead to the same cycles. For example, we integrated each of 3 particular networks from 20 different (randomly generated) initial conditions and found that trajectories from 14 of the initial points converged on a length-110 cycle in one network; 11 of the initial points converged on a length-252 cycle in the second network; and all 20 initial points converged on a length-174 cycle in the third.

Bistability and multistability are possible in Boolean 4-nets, though we did not look for it in our random sample. It is clearly possible to have two stable fixed points even in a 2- or 3-net [e.g., Fig. 1(a)], or to have a stable fixed point and a stable periodic orbit in a 4-net. It is also possible to have two stable periodic orbits in a 4-net. A simple possibility is that of two isolated cycles of length 4. Such cycles can have stable periodic orbits if the focal points are not all ± 1 .¹¹ The example in Fig. 7 is more interesting. It has two stable periodic orbits (proven by methods in Sec. IV) which share part

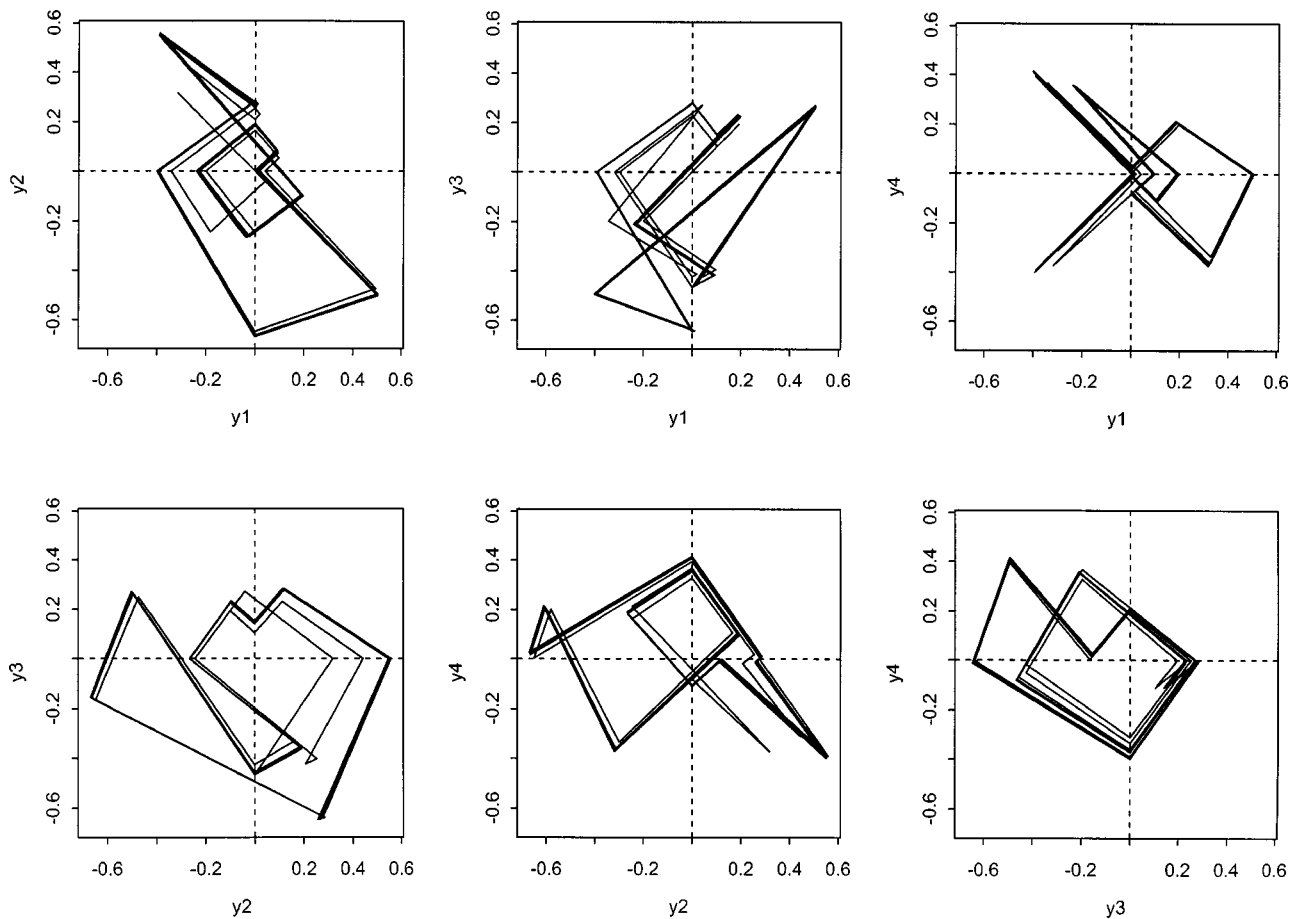


FIG. 6. Phase space projections of a periodic orbit with switching sequence of length 110 on the 4-net of Fig. 5. Note that the amplitude of this cycle is much larger than for the cycle of length 174 in Fig. 4.

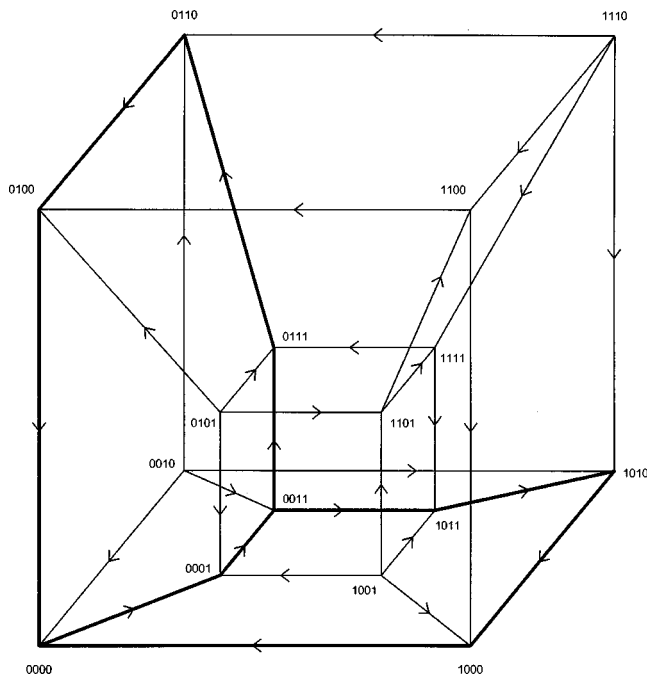


FIG. 7. Hypercube structure of a 4-net with two stable periodic orbits following cycles marked by bold lines.

of their path on the 4-cube, namely

$$0000 \rightarrow 0001 \rightarrow 0011 \rightarrow 1011 \rightarrow 1010 \rightarrow 1000$$

and

$$0000 \rightarrow 0001 \rightarrow 0011 \rightarrow 0111 \rightarrow 0110 \rightarrow 0100.$$

In this case, both orbits are equivalent to the three-dimensional cyclic attractor shown in Fig. 1(b), and have the same period, 2.8872710.

VI. CLASSES OF CYCLES

One way to classify cycles is by their periods, as in the results of the random networks reported above. Another is by switching sequences, which do not correspond one-to-one with periods. Many different switching sequences may have the same period, and a given switching sequence may correspond to periodic orbits with different periods. To specify completely a cycle on a directed graph on the 4-cube, it is necessary to give both the switching sequence and the pattern of alternate exit variables, i.e., directions of edges adjacent to the cycle. Thus, a given switching sequence may belong to more than one different periodic orbit (with different period), depending on the pattern of adjacent edges.

However, symmetries imply that apparently different switching sequences may be structurally the same.¹⁶ Relabeling the variables or changing the starting point of the cycle will give an apparently different sequence that is nevertheless structurally unchanged. This is still true when adjacent edges are taken into account. One way to extract the structure of a switching sequence is to use the "interval sequence."¹⁶ The interval sequence gives the number of intervening digits in the switching sequence between consecutive occurrences of each variable. However, the interval sequence is still not a unique identifier, in that more than one

TABLE V. Canonical switching sequences of length 8.

Switching sequence	Interval sequence
12121313	(15)(15)(1111)
12123434	(15)(15)(15)(15)
12131213	(33)(33)(1111)
12132434	(15)(15)(24)(24)
12134234	(15)(24)(24)(33)
12134243	(15)(15)(33)(33)
12314234	(24)(24)(33)(33)
12314324	(24)(24)(24)(24)
12341234	(33)(33)(33)(33)

structure may have the same interval sequence (consider a sequence and its reverse, which we must consider as different sequences).

Another way to identify structurally identical switching sequences is to transform each sequence into a canonical form, unique for its equivalence class. The simplest way to do this is to find the member of an equivalence class that is lexicographically minimal, or in this context, smallest considered as an integer. For example, the sequences

$$1213124314 \quad \text{and} \quad 1213421413$$

are structurally equivalent, the first being the canonical form for this class. (To transform the second to canonical form, change 2's to 3's and vice versa and start from the second-to-last digit in the sequence.)

Structurally distinct switching sequences were listed long ago by Gilbert²⁷ but he counts only elementary cycles (those that pass through each vertex only once) and does not consider cycles traversed in opposite directions to be distinct. The sequence of length 10 above, for example, has a different canonical form when reversed. There is one canonical switching sequence of length 4 (1212) and there are two of length 6 (121323 and 123123). Table V lists the nine possible canonical forms of switching sequences of length 8.

All but the first two (which are not elementary cycles) are as listed by Gilbert. According to our present definition of equivalence, we find 33 canonical forms for switching sequences of length 10, rather than the 10 given by Gilbert. In our random sample of 1000000 networks, the 8322 stable periodic orbits that we found represent 370 different canonical switching sequences.

For a given switching sequence there are many possible arrangements of adjacent edge orientations, but most of these we do not expect to correspond to periodic orbits. For example, for the sequence 123123 on the 3-cube there are 6 adjacent edges and therefore 2^6 different patterns of adjacent edge orientations. Many of these are equivalent by symmetry, but in the end only one of these patterns gives a cycle with a periodic orbit, namely, the one with all adjacent edges pointing inwards to the cycle, i.e., the cyclic attractor. (This is not true, of course, for the more general class of switching networks with focal points not necessarily at ± 1 .) To illustrate a class of cycles on the 4-cube with a given switching sequence, consider Fig. 8. This has a cycle that is not quite a cyclic attractor, since there is a chord from (0111) to (0101) and since the edge (0110) \rightarrow (1110), which is adjacent to the

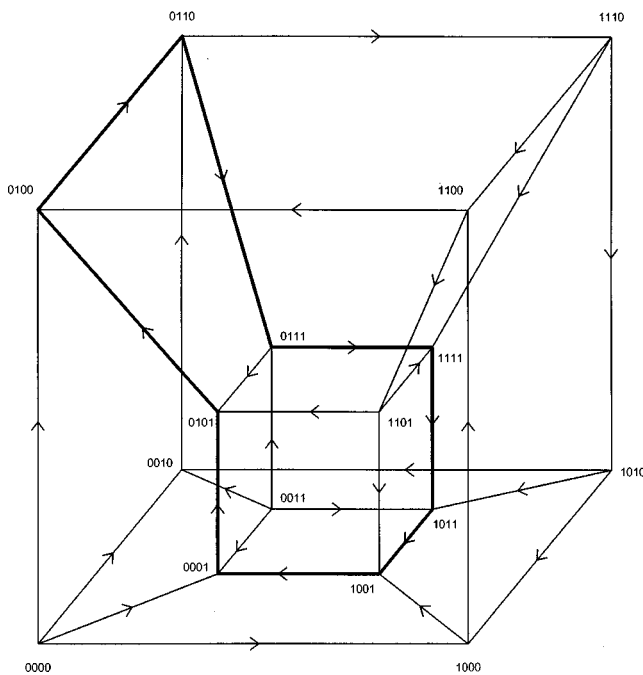


FIG. 8. A cycle on a 4-cube with switching sequence 43412312, having a stable periodic orbit. Reversing some of the edges that point inward toward the cycle can still produce a periodic orbit, but with a different period.

cycle, points away from the cycle. Everywhere else, adjacent edges point inwards to the cycle. The switching sequence for this cycle is 43412312, which has canonical form 12134234 and the methods of Sec. IV can be used to show that the cycle corresponds to a stable periodic orbit of period ≈ 3.763906 . If the edge $(0110) \rightarrow (1110)$ is reversed, so that it also points in towards the cycle, then no periodic orbit exists for the cycle. [Intuitively, $(0110) \rightarrow (1110)$ needs to point outward, i.e., y_1 has to be pulled in the positive direction, so that at the next step the chord is not followed, but $(0111) \rightarrow (1111)$.]

However, some of the adjacent edges that point in towards the cycle (or some combinations of several) can be turned outwards and still leave a stable periodic orbit for the resulting cycle. There are 14 adjacent edges to this cycle, excluding the chord, and so 2^{14} patterns of adjacent edge orientations for each orientation of the chord. There are no symmetries for this cycle to reduce this number of patterns. Leaving the direction of the chord as depicted, 15 different patterns of adjacent edge orientations give stable periodic orbits. These are listed in Table VI where edges are specified by their endpoint vertices expressed as decimal equivalents of their binary labels. Thus, the edge from (1011) to (1010) is written $11 \rightarrow 10$. Cycles with other inward-pointing adjacent edges turned out do not have corresponding periodic orbits. If the chord is reversed, another set of 31 different cycles with stable periodic orbits (3 of them degenerate) occur (Table VII). In addition, we can reverse more edges and end up with an unstable cycle, e.g., without the chord reversed, reversing $1 \rightarrow 0$, $5 \rightarrow 13$, $6 \rightarrow 2$, and $15 \rightarrow 13$ to give a cycle with an unstable periodic orbit of period 0.957001.

Thus, each possible switching sequence may have a siz-

TABLE VI. Edge reversal patterns producing stable period orbits for the cycle in Fig. 8 (binary vertex labels are represented by their decimal equivalents).

Edges reversed		Period	
none		3.763906	
11 → 10		3.552914	
9 → 8		3.302676	
1 → 0		2.936174	
6 → 2		2.958148	
7 → 3		3.137461	
11 → 10,	6 → 2	2.712756	
11 → 10,	7 → 3	2.936174	
9 → 8,	6 → 2	2.437511	
9 → 8,	7 → 3	2.712756	
1 → 0,	5 → 13	2.854426	
1 → 0,	6 → 2	1.968397	
1 → 0,	7 → 3	2.372957	
1 → 0,	5 → 13,	6 → 2	1.691689
1 → 0,	5 → 13,	7 → 3	2.580393

able set of periodic orbits associated with it, determined by the adjacent edge orientations.

In some cases relationships between networks can be understood from structural principles. For example, consider a 4-element network in which one element has no outputs to other elements (e.g., y_i does not depend on \tilde{y}_4 for $i \neq 4$). In

TABLE VII. Edge reversal patterns producing stable period orbits for the cycle in Fig. 8 with the chord, $5 \rightarrow 7$, reversed (binary vertex labels are represented by their decimal equivalents).

Edges reversed	Period
9 → 8	2.887271
1 → 0	2.887271
9 → 8, 4 → 0	2.712756
9 → 8, 4 → 12	2.528355
9 → 8, 6 → 2	2.712756
9 → 8, 6 → 14	3.122078
1 → 0, 5 → 13	2.712756
1 → 0, 6 → 2	2.292432
1 → 0, 6 → 14	3.418036
1 → 0, 7 → 3	2.292432
9 → 8, 4 → 0, 4 → 12	2.292432
9 → 8, 4 → 0, 6 → 2	2.538797
9 → 8, 4 → 0, 6 → 14	2.978774
9 → 8, 4 → 12, 6 → 2	2.292432
9 → 8, 4 → 12, 6 → 14	2.887271
9 → 8, 6 → 2, 6 → 14	2.978774
1 → 0, 5 → 13, 6 → 2	1.968397
1 → 0, 5 → 13, 6 → 14	3.302676
1 → 0, 5 → 13, 7 → 3	2.372957
1 → 0, 4 → 12, 6 → 14	2.887271 (degenerate)
1 → 0, 6 → 2, 6 → 14	3.122078
1 → 0, 7 → 3, 15 → 13	1.443635
9 → 8, 4 → 0, 4 → 12, 6 → 2	2.094713
9 → 8, 4 → 0, 4 → 12, 6 → 14	2.712756
9 → 8, 4 → 0, 6 → 2, 6 → 14	2.830288
9 → 8, 4 → 12, 6 → 2, 6 → 14	2.712756
1 → 0, 5 → 13, 6 → 2, 6 → 14	2.958148
1 → 0, 4 → 12, 6 → 2, 6 → 14	2.292432 (degenerate)
1 → 0, 4 → 12, 6 → 14, 7 → 3	2.292432 (degenerate)
9 → 8, 4 → 0, 4 → 12, 6 → 2, 6 → 14	2.538797
1 → 0, 4 → 12, 6 → 14, 7 → 3, 15 → 13	1.443635

this case, the dynamics of the network are essentially three-dimensional, with y_4 being driven by the other three. However, if the 3 driving elements oscillate, y_4 may still switch and then the cycle on the 4-cube will not simply be the 3-cube cycle [Fig. 1(b)] embedded into the 4-cube. It is not always so easy, however, to see an underlying simpler structure in a complicated cycle.

VII. DISCUSSION

This work blends combinatorics and nonlinear dynamics to explore the properties in a class of piecewise linear differential equations that model genetic and other networks in which switchlike interactions are believed to dominate the observed behaviors. The surprising result is that as the networks become larger there is an astronomical increase in the total number of different networks as defined by distinct configurations in directed n -cubes that capture network structures. Thus, in 3 dimensions there are 112 different networks, in 4 dimensions there are 10^7 different networks, and in 5 dimensions there are 3×10^{20} different networks. Although we have not counted the number of distinct cycles or distinctly different chaotic dynamics in these networks, the current results indicate that there are thousands of different networks that show interesting (i.e., limit cycles or chaos) dynamics. Cycles are related to one another. For example, flipping a single edge in a network with a stable cycle often yields another stable cycle, with different dynamic properties. Thus, many configurations leading to stable cycles may arise from small “mutations” in the network structure. Other “mutations” might lead to other sorts of behaviors such as steady states or chaos.

This work raises a large number of intriguing questions of a mathematical nature. We mention several.

- (1) For a given dimension, n , what is the longest stable cycle (in period and symbolic sequence) for networks in which the focal points are at ± 1 ?
- (2) For a given dimension, n , what is largest number of stable attractors in a network for networks in which the focal points are at ± 1 ? (It is easy to see that there is always a network with 2^{n-1} stable nodes.)
- (3) As the positions of the focal points in a network vary, what are the generic ways in which stable attractors undergo bifurcations?
- (4) For a given network, what possible behaviors can be found as a function of the position of the focal points?

The extent to which analysis of the current equations is pursued will likely depend on the perceived relevance of these equations to model real or artificial genetic networks.

The current networks are appropriate to analyze asynchronous switching networks. Although hypercube mappings of dynamics were initially used in this context,²⁸ we are not aware of exploitation of these methods in recent years. Nevertheless, given the simple structure of these networks, their synthesis *in silico* would be comparatively straightforward. Certainly it would be interesting to build analog networks and study their dynamics using the theoretical methods outlined here.

A more provocative issue is whether the current methods are really appropriate to model real genetic networks found in nature. The current version of Eq. (1) does not incorporate many factors that are important in the biological context including: spatial structure, time delays associated with transcription and translation, differences in threshold for the same transcription factor at different loci, sigmoidal rather than steplike changes in control of synthesis, variable decay rates for different transcription factors. Although such factors could be easily incorporated by modifying the current equations, the mathematical transparency of the current formulation would be lost.

Despite these potential objections to the current approach, two factors stand out. First, molecular biologists still think of genes as being switched “on” or “off” based on the presence or absence of the controlling transcription factors (which at the current time are the focus of intense study in particular gene expression circuits). Second, even though it was demonstrated long ago that the current equations could generate a bistable toggle switch and stable oscillations (Fig. 1), it was not until 27 years later that networks having these dynamics were synthesized out of genetic components.^{29,30} Thus, the path has been set to synthesize networks *in vitro*, out of genetic components having predetermined logical structure and dynamical behavior.

The current work places the analysis of genetic networks in a combinatorial context. Thus, this work may be helpful in classifying and identifying genetic networks based on their dynamics and on their logical structure. Moreover, since mutations in biological systems are associated with discrete events (e.g., change of a single base pair, transposition of two segments of chromosome, deletion of a segment of a chromosome), the current work offers novel ways to think about the ways mutations can lead to altered dynamics in genetic networks. It also offers a huge repertoire of dynamics that might be possible using genetic components. Finally, the enormous explosion in information about the structure of the genome in man and other organisms will require new methods of analysis to help understand the orderly functioning of the genetic networks underlying life.

ACKNOWLEDGMENTS

We thank NSERC for partial support of this research, and one of our reviewers for the reference to the paper by Chen.

APPENDIX

We wish to count the number of distinct digraphs on the n -cube. We first review the construction of the group of symmetry transformations.

It is known that the group of symmetries, O_n , consists of signed permutations. We formulate this result as follows. The vertices of the n -cube are labeled by n -bit binary codes (e.g., see Fig. 1), or equivalently, n -vectors with components ± 1 . We can think of each transformation as a choice of which vertex will be taken to the $(+, +, \dots, +)$ position and then a choice of permutation of the n variables (vector components) corresponding to a permutation of the edges

adjacent to the $(+, +, \dots, +)$ vertex. Each transformation can be represented, therefore, as a matrix PS , where S is a signature similarity matrix (a diagonal matrix with diagonal entries ± 1) and P is a permutation matrix. To verify that these matrices PS exactly correspond to the desired symmetry transformations, first note that there are clearly 2^n S matrices and $n!$ P matrices. It is easy to check that if $P_1 S_1 \mathbf{v} = P_2 S_2 \mathbf{v}$ for all vertex vectors \mathbf{v} , then $P_1 = P_2$ and $S_1 = S_2$, so that all the PS matrices are genuinely different transformations. Also, each PS matrix is a valid transformation in the sense that it preserves the adjacency structure of vertices. Adjacent vertices are those whose label vectors differ in exactly one bit (or component), and if \mathbf{v} and \mathbf{w} are vertex vectors that differ in the j th bit, then $PS(\mathbf{v}) - PS(\mathbf{w}) = PS(\mathbf{v} - \mathbf{w}) = PS(\pm \mathbf{e}_j) = \pm \mathbf{e}_k$ for some k .

For each choice of PS we need to count the number of digraphs left invariant. Let a_k denote (undirected) edges of the graph and let T represent a transformation PS so that if a_1 is the edge between vertices \mathbf{v} and \mathbf{w} , then $T(a_1)$ is the edge between vertices $PS\mathbf{v}$ and $PS\mathbf{w}$. Then, the edges of the graph will be grouped into cycles such as, e.g., $T(a_1) = a_2, T(a_2) = a_3, T(a_3) = a_1$ and $T(a_4) = a_5, T(a_5) = a_4$ and also possibly $T(a_6) = a_6$. Now, in order to count invariants, we note that for each such cycle there is a single choice of edge orientation. In the example just given, we can select the orientation of the edge a_1 (2 ways) but then if the graph is to be invariant under the transformation T , the orientation of a_2 is determined by that of a_1 since $T(a_1) = a_2$, and then the orientation of a_3 is determined by that of a_2 and so on around the cycle. Thus, the number of choices of invariant graphs under T is $I(T) = 2^d$, where d is the number of edge cycles induced by T . It is also possible that $T^j(a_1) = a_1$ for some j but that the vertices get reversed under this transformation, i.e., $(PS)^j \mathbf{v} = \mathbf{w}$ and $(PS)^j \mathbf{w} = \mathbf{v}$, where \mathbf{v} and \mathbf{w} are adjacent. In such a case, no invariant digraphs are possible for this transformation, since at least one edge must be reversed under T . The number of cycles, d , for a given transformation, T , can be computed in a brute force manner according to the following algorithm:

```

d = 0
nedge = n2^{n-1}
for (k = 1 to nedge) edge_visited[k]
  = ``false``
for (k = 1 to nedge) {
  if (NOT(edge_visited[k])) {
    d = d + 1
    edge_visited[k] = ``true``
    new_edge = T(a_k)
    while (new_edge ≠ a_k) {
      edge_visited[new_edge] = ``true``
      new_edge = T(new_edge)
    }
    if (new_edge is reverse of a_k) {
      d = 0
      break
    }
  }
}

```

Note that if the final if-block is removed (i.e., we allow reversal of edges within the equivalence relation), we get the count of cycles for the edge-coloring problem considered by Chen.²⁵

The number of equivalence classes can be computed by looping through the possible transformations $T_i, i = 1, \dots, m(n)$ (i.e., the possible pairs of matrices P and S), computing the number of cycles $d(T_i)$ for each transformation, and counting how many transformations there are, $\nu(d)$, for each value of d . This gives Eq. (5),

$$c(n) = \frac{1}{m(n)} \sum_d \nu(d) 2^d = \frac{\sum_d \nu(d) 2^d}{n! 2^n}$$

as desired.

- ¹S. A. Fodor, "Massively parallel genomics," *Science* **277**, 393–395 (1997).
- ²R. Sapolsky, L. Hsie, A. Berno, G. Ghandour, M. Mittmann, and J. B. Fan, "High-throughput polymorphism screening and genotyping with high-density oligonucleotide arrays," *Genetic Analysis: Biomolecular Engineering* **14**, 187–192 (1999).
- ³D. Thieffry and R. Thomas, "Dynamical behavior of biological regulatory networks. II. Immunity control in bacteriophage lambda," *Bull. Math. Biol.* **57**, 277–295 (1995).
- ⁴H. H. McAdams and L. Shapiro, "Circuit simulation of genetic networks," *Science* **269**, 650–656 (1995).
- ⁵J. Reintz and D. H. Sharp, "Mechanism of *eve* stripe formation," *Mechanisms of Development* **49**, 133–158 (1995).
- ⁶L. Mendoza and E. Alvarez-Buylla, "Dynamics of the genetic regulatory network for *Arabidopsis thaliana* flower morphogenesis," *J. Theor. Biol.* **193**, 307–319 (1998).
- ⁷S. A. Kauffman, "Metabolic stability and epigenesis in randomly constructed genetic networks," *J. Theor. Biol.* **22**, 437–467 (1969).
- ⁸S. A. Kauffman, *Origins of Order: Self-Organization and Selection in Evolution* (Oxford University Press, Oxford, 1993).
- ⁹R. Thomas and R. D. Àri, *Biological Feedback* (Chemical Rubber, Boca Raton, 1990).
- ¹⁰L. Glass, "Classification of biological networks by their qualitative dynamics," *J. Theor. Biol.* **54**, 85–107 (1975).
- ¹¹L. Glass and J. S. Pasternack, "Stable oscillations in mathematical models of biological control systems," *J. Math. Biol.* **6**, 207–223 (1978).
- ¹²T. Mestl, E. Plahte, and S. W. Omholt, "Periodic solutions in systems of piecewise-linear differential equations," *Dyn. Stab. Sys.* **10**, 179–193 (1995).
- ¹³T. Mestl, C. Lemay, and L. Glass, "Chaos in high-dimensional neural and gene networks," *Physica D* **98**, 33–52 (1996).
- ¹⁴R. Edwards, "Chaos in a continuous-time Boolean network," in *Proceedings of the Third International Conference on Dynamic Systems and Applications*, Atlanta, May–June, 1999 (in press).
- ¹⁵R. Edwards, "Analysis of continuous-time switching networks," *Physica D* (in press).
- ¹⁶L. Glass, "Combinatorial aspects of dynamics in biological systems," in *Statistical Mechanics and Statistical Methods in Theory and Application*, edited by U. Landman (Plenum, New York, 1977), pp. 585–611.
- ¹⁷L. Glass and S. A. Kauffman, "The logical analysis of continuous nonlinear biochemical control networks," *J. Theor. Biol.* **39**, 103–129 (1973).
- ¹⁸L. Glass and J. S. Pasternack, "Prediction of limit cycles in mathematical models of biological oscillations," *Bull. Math. Biol.* **40**, 27–44 (1978).
- ¹⁹E. Plahte, T. Mestl, and S. W. Omholt, "Global analysis of steady points for systems of differential equations with sigmoid interactions," *Dyn. Stab. Syst.* **9**, 275–291 (1994).
- ²⁰J. E. Lewis and L. Glass, "Steady states, limit cycles, and chaos in models of complex biological networks," *Int. J. Bifurcation Chaos Appl. Sci. Eng.* **1**, 477–483 (1991).
- ²¹J. E. Lewis and L. Glass, "Nonlinear dynamics and symbolic dynamics of neural networks," *Neural Comput.* **4**, 621–642 (1992).
- ²²D. Slepian, "On the number of symmetry types of Boolean functions of n variables," *Can. J. Math.* **5**, 185–193 (1953).

- ²³S. W. Golomb, "A mathematical theory of discrete classification," in *Information Theory: Fourth London Symposium*, edited by C. Cherry (Butterworth, London, 1961), pp. 404–423.
- ²⁴C. E. Shannon, "The synthesis of two-terminal switching circuits," *Bell Syst. Tech. J.* **28**, 59–98 (1949).
- ²⁵W. Y. C. Chen, "Induced cycle structures of the hyperoctahedral group," *SIAM (Soc. Ind. Appl. Math.) J. Disc. Math.* **6**, 353–362 (1993).
- ²⁶A. Berman and R. J. Plemmons, *Nonnegative Matrices in the Mathematical Sciences* (Academic, New York, 1979).
- ²⁷E. N. Gilbert, "Gray codes and paths on the n -cube," *Bell Syst. Tech. J.* **37**, 815–826 (1958).
- ²⁸W. Keister, A. E. Ritchie, and S. H. Washburn, *The Design of Switching Circuits* (Van Nostrand, Toronto, 1951), pp. 172–175.
- ²⁹M. B. Elowitz and S. Leibler, "A synthetic oscillatory network of transcriptional regulators," *Nature (London)* **403**, 335–338 (2000).
- ³⁰T. S. Gardner, C. R. Cantor, and J. J. Collins, "Construction of a genetic toggle switch in *Escherichia coli*," *Nature (London)* **403**, 339–342 (2000).